

Article

Accuracy of Modified Johnson–Cook Modelling of the Blanking Process through Experimental and Numerical Analysis

Lotfi Ben Said ^{1,2,*} , Taoufik Kamoun ³, Hamdi Hentati ^{4,5} and Mondher Wali ^{2,5} 

¹ Department of Mechanical Engineering, College of Engineering, University of Ha'il, Ha'il City 2440, Saudi Arabia

² Laboratory of Electrochemistry and Environment (LEE), National Engineering School of Sfax, University of Sfax, Sfax 5080, Tunisia

³ Higher Institute of Technological Studies of Sfax, Sfax 3099, Tunisia

⁴ Laboratory of Mechanics Modeling and Production, National Engineering School of Sfax, University of Sfax, Sfax 5080, Tunisia

⁵ Higher School of Sciences and Technology of Hammam Sousse, University of Sousse, Sousse 4002, Tunisia

* Correspondence: bensaid_rm@yahoo.fr

Abstract: Metal parts undergo a blanking test that involves experimentation with different process parameters across multiple levels. The presence of uncontrolled burrs (measured as Hbv) significantly affects the precise geometry of the blanked parts, making it a primary concern in precision blanking. Moreover, the maximum blanking force (F_{max}) holds considerable significance, as it aids in forecasting fracture mechanisms and plays a pivotal role in the design of blanking tools. The aim of this study is to assess the predictive capabilities of an elasto-plastic model coupled with damage in capturing the behavior of sheet material during the blanking process. Additionally, integrating the rate-dependent aspect into the model is crucial for accurately modeling the mechanical behavior of sheet metal. Our focus remains on demonstrating the efficacy of the model in predicting blanking force and burr formation. The numerical model incorporates modified plasticity and damage Johnson–Cook models to achieve this objective, considering the combined effect of strain and strain rate fields in the sheet blanking process. Experimental validation proves the efficacy of the proposed model in accurately predicting blanking outcomes. The experimental results confirm the model's capability to provide a consistent prediction of the blanking force and burr dimensions. In addition, it was proved experimentally that the sheet thickness has the most influence on Hbv and F_{max} .

Keywords: blanking tests; modified Johnson–Cook models; ductile fracture; combined friction model

MSC: 70-10



Citation: Ben Said, L.; Kamoun, T.; Hentati, H.; Wali, M. Accuracy of Modified Johnson–Cook Modelling of the Blanking Process through Experimental and Numerical Analysis. *Mathematics* **2024**, *12*, 1209. <https://doi.org/10.3390/math12081209>

Academic Editors: Shujin Laima, Xiaowei Jin, Hehe Ren and Yong Cao

Received: 21 March 2024

Revised: 9 April 2024

Accepted: 16 April 2024

Published: 17 April 2024



Copyright: © 2024 by the authors. Licensee MDPI, Basel, Switzerland. This article is an open access article distributed under the terms and conditions of the Creative Commons Attribution (CC BY) license (<https://creativecommons.org/licenses/by/4.0/>).

1. Introduction

In contrast to forming processes [1–3], where the purpose is to deform plastically the metal without fracture, metal cutting processes lead to the total rupture of the workpiece [4,5]. Different experimental and numerical analyses were carried out in order to determine optimal manufacturing parameters. The optimization of these manufacturing processes, like additive manufacturing [6,7], machining and blanking [8–10], and other processes [11,12], has a significant impact on the quality of products. These studies focus on the influence of input manufacturing parameters principally on the geometric aspects and on the maximum force that causes total failure of workpieces. Metal cutting is an essential operation such as blanking and machining that precedes many metal working processes. The precision of the workpiece geometry sample is usually important for the final product results.

The blanking process is considered as one of the most-used methods in manufacturing [13]. The present work investigates the effect of cutting parameters on the sheet

blanking process using numerical and experimental studies. The blanking process is based on the applied pressure of the punch and the die on the sheet metal. Currently, the right blanking parameters for a new product are determined empirically by carrying out many experimental tests. Despite the growth of blanking technology in terms of cutting methods and tools design, there is still a lack of optimal models of blanking processes. A complex stress distribution is reached on a blanking operation.

On the numerical scale, steel sheet finite element analysis was conducted to explore ductile failure mechanisms in the fine-blanking process [14]. This involved using a modified GTN model [15] that integrates Lemaitre's damage mechanics approach [16] with the Gurson void damage model [17]. A metallographic analysis was carried out to understand the evolution of damage. This involved analyzing the fracture propagation, with numerical findings aligning well with the experimental results from the fine-blanking process. The study emphasizes the significance of investigating process parameters like clearance, die, and punch diameters. In the same context, various finite element approaches have emerged to simulate the blanking process [18,19], differing primarily in their methods for modeling material failure. Both mechanical and thermomechanical numerical models have been developed. The thermal term in plasticity and damage models is recommended based on experimental and numerical tests for simulating bar blanking. However, the efficacy of the mechanical model in computing blanking operations remains a point of consideration.

In another context, experimental investigations were conducted, aiming to analyze the effects of clearance, friction, and cutting parameters on the resulting geometrical quality of the product, as well as the formation and growth of burrs along the sheet edge [20,21]. Some researchers are directing their attention toward studying how various blanking parameters specifically affect the wear and tear of the punch used in the process [22,23]. Actually, the extent of tool wear is contingent upon factors such as the specific clearance value employed, the material constituting the punch, and the hardness of the blank pieces being processed [24,25]. Further investigations [26,27] indicate that the size of the burr depends on several factors, including the tool edge's wear condition, the clearance employed in blanking, and the inherent properties of the materials used in the process. These studies have substantiated that wear facilitates the presence of burrs, and the clearance setting significantly influences both the fracture angle within the sheet metal's shear zone and the resultant burr height. Therefore, it becomes imperative to determine experimentally the size of the burrs on the sheet pieces. Evaluating the quality of the products is intricately tied to estimating the acceptable level of burr on these parts.

Furthermore, Johnson–Cook plasticity and damage models [28,29] are extensively employed as numerical tools to simulate material behavior and failure during blanking processes. These models primarily aim to assess a material's ability to withstand deformation until reaching failure points. However, most of the literature overlooks the strain rate dependency during blanking processes. However, as the blanking speed increases, there is a noticeable deviation between the numerical predictions and the experimental results [30]. This could be attributed to thermal softening and variations in material parameters, which were determined through conducting various tensile tests with varying strain rates.

This study aims to evaluate the predictive capabilities of Johnson–Cook plasticity and cumulative-damage fracture models, which express the strain to fracture as a function of strain rate, in capturing the behavior of sheet material during the blanking process. Numerical simulations are conducted based on a rate-dependent elasto-plastic constitutive model combined with a fracture criterion to predict the maximum blanking force and blanking burr dimensions. The Johnson–Cook parameters are determined from experimental tensile tests conducted at different strain rates. The accuracy of the developed model is validated through experimental studies. A comparison between the numerical and experimental results of sheet blanking tests confirms that incorporating modified Johnson–Cook models accounting for the strain rate term is essential for accurately predicting the behavior and damage of S235 sheet steel during blanking operations.

2. Experiments and Methods

The adopted material for this experimental study is S235 steel. The chemical composition of the studied material is presented in Table 1.

Table 1. Specification of the S235 steel grade [3].

%C	%Mn	%P	%S	%Si
0.22 max	1.6 max	0.05 max	0.05 max	0.05 max

Initially, stress–strain curves are experimentally acquired to determine the mechanical characteristics and response of the sheet metal under tensile loading. The samples are subjected to a uniaxial tensile test until reaching failure at ambient temperature, as illustrated in Figure 1. An extensometer is used in tensile testing to provide direct strain measurements on the specimen.

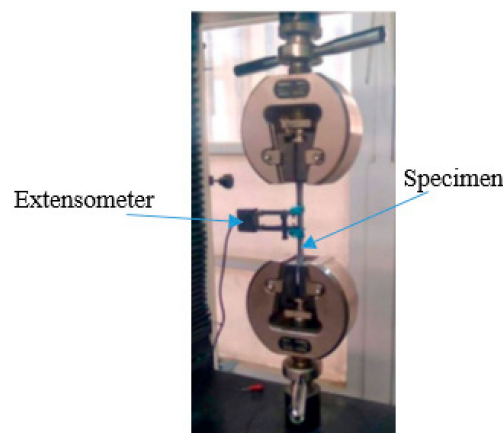


Figure 1. Experimental set-up of tensile test.

After that, blanking tests are elaborated in the same tensile machine with a specific tool. Figure 2a,b show the tool and the sheet strip used in our experimental tests and the 3D design of the used blanking tool, respectively. In the experimental blanking test, the sheet metal is put on the die. The punch moves down and presses the sheet until fracture.

It was found in previous experimental studies of the blanking process that the maximum blanking force (F_{max}) and the blanking burr (Hbv) are affected mainly by the sheet thickness (t), clearance (c), and punch diameter (d) [23,31,32].

The values of the blanking parameters are presented in Table 2.

Table 2. Blanking parameters.

Blanking Parameters	Sheet Thickness Th (mm)		Punch Diameter D (mm)		Speed S_p (mm/min)		Clearance J (%)	
	1	2	14	18	20	40	10	20
Value	1	2	14	18	20	40	10	20

Two tools and four dies were considered, corresponding to two different diameters and two clearances, which correspond to the most-used clearances in industry, $J = 10\%$ and $J = 20\%$.

The clearance is expressed as follows:

$$J(\%) = 100 \cdot \frac{D_{die} - D}{2 \cdot Th} \tag{1}$$

where D_{die} is the die diameter.

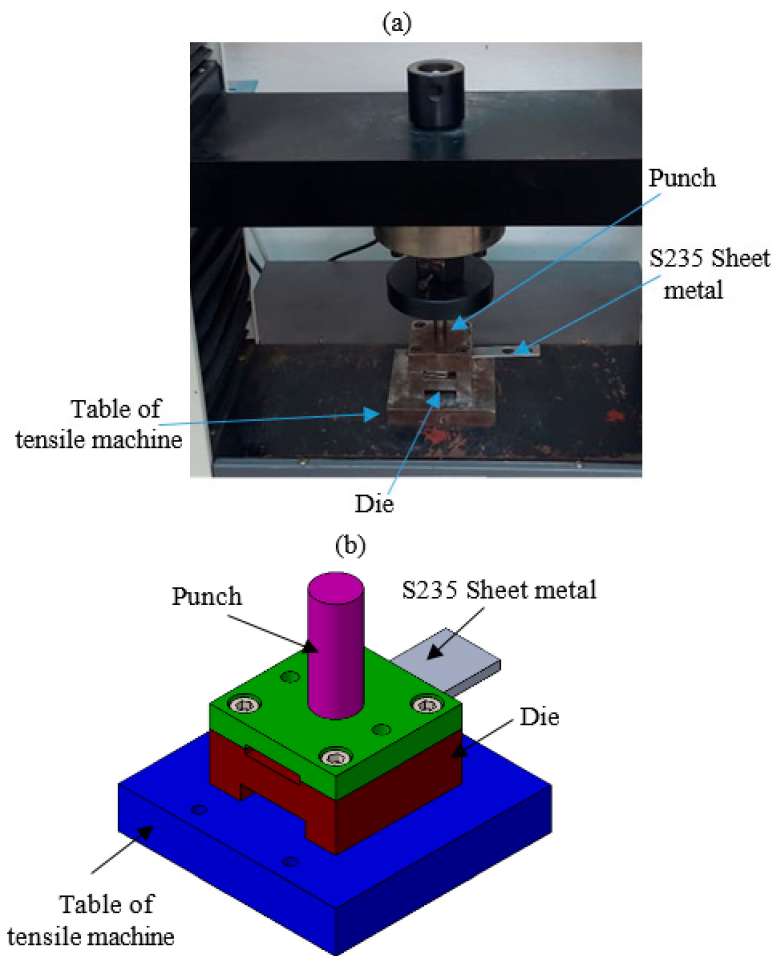


Figure 2. Experimental blanking tool: (a) tools and strip during blanking test; (b) 3D design of blanking tool.

3. Plasticity and Damage Models of Blanking Operation

3.1. Constitutive Model of Plasticity: Rate-Dependent Model

The rational stress–strain relationship, also known as the true stress–strain equation, is derived to facilitate a finite element simulation of blanking operations. This equation is obtained from the engineering stress–strain curve, also known as the conventional stress–strain curve, which tracks stress changes with strain until the specimen bifurcates.

The true stress σ_v and true strain ε_v are defined by the following equation:

$$\begin{aligned}\sigma_v &= \frac{F}{S} = \sigma(1 + \varepsilon) \\ \varepsilon_v &= \int_{L_0}^L \frac{dL}{L} = \ln(1 + \varepsilon)\end{aligned}\quad (2)$$

where σ and ε are, respectively, the engineering stress and the engineering strain terms, F is the applied force, S is the instantaneous cross-sectional area of the tensile specimen, and L_0 and L are the original and the current length of the gauge section, respectively. A good understanding of mechanical properties is essential for efficient numerical modeling of the sheet cutting and sheet forming processes. Various empirical formulations have been outlined to compute the elastoplastic deformation characteristics of sheet metal during these operations [18]. Moreover, when strength is influenced by the strain rate parameter, the plasticity law becomes rate-dependent. It is essential to consider the strain rate sensitivity in both the plasticity and damage laws associated with sheet blanking processes. Conversely, the effects of thermal softening can be ignored. To address this, the modified Johnson–Cook

law (Equation (3)) [28] was devised and commonly employed to characterize the ductile material response under strain hardening and strain rate hardening.

$$\sigma_{eq} = \left(A + B \left(\varepsilon_{pl} \right)^n \right) \left(1 + C \operatorname{Ln} \left(\frac{\dot{\varepsilon}}{\dot{\varepsilon}_0} \right) \right) \tag{3}$$

The modified Johnson–Cook law describes the strain hardening effect in materials, where it depends on four key parameters denoted as A , B , n , and C . These parameters correspond to the yield stress, the strain hardening coefficients, and a material property influencing the strain rate sensitivity, respectively.

Firstly, the materials constants A , B , and n are identified based on this relationship:

$$\sigma_{eq} = \left(A + B\varepsilon_{pl}^n \right) \tag{4}$$

This plasticity law (Equation (3)) establishes the correlation between strain and stress. By applying the logarithm function to this equation [2], we derive a linear relationship (Equation (4)), which serves as the foundation for calibrating the flow stress model through experimental tensile testing.

$$\operatorname{Ln}(\sigma_{eq} - A) = n \operatorname{Ln}(\varepsilon_{pl}) + \operatorname{Ln}(B) \tag{5}$$

Subsequently, this calibration allows us to predict accurately the strain hardening parameters.

Secondly, the material constant C may be determined. In fact, the relationship (Equation (2)) can be represented as Equation (6) [2].

$$\frac{\sigma_{eq}}{\left(A + B \left(\varepsilon_{pl} \right)^n \right)} = \left(1 + C \operatorname{Ln} \left(\frac{\dot{\varepsilon}}{\dot{\varepsilon}_0} \right) \right) \tag{6}$$

Then, the term $\frac{\sigma_{eq}}{\left(A + B \left(\varepsilon_{pl} \right)^n \right)}$ in the function $\operatorname{Ln} \left(\frac{\dot{\varepsilon}}{\dot{\varepsilon}_0} \right)$ should be illustrated as a linear curve.

Once the strain hardening parameters are identified and the data points are fitted accordingly, a linear fitting is performed utilizing a first-order regression model. We can then determine the strain rate dependence coefficient, C .

3.2. Constitutive Model of Ductile Damage: Rate-Dependent Model

The decrease in strength property is intricately related to the relationship between the damaged stress, denoted σ_D , and the damage parameter, represented as D . This relationship is mathematically expressed in Equation (7).

$$\sigma_D = (1 - D)\sigma_{eq}; 0 \leq D \leq 1 \tag{7}$$

In addition, advanced numerical models consider the impact of stress triaxiality, represented by η , on the evolution of strain damage (Equation (8)) [4,11].

$$\eta = \frac{\sigma_H}{\sigma_{eq}} = \frac{\frac{\sigma_I + \sigma_{II} + \sigma_{III}}{3}}{\sqrt{\frac{1}{2} \left[(\sigma_I - \sigma_{II})^2 + (\sigma_{II} - \sigma_{III})^2 + (\sigma_{III} - \sigma_I)^2 \right]}} \tag{8}$$

This triaxiality factor serves as a dimensionless ratio that compares the hydrostatic stress to the Von Mises equivalent stress. The damage model used in blanking processes is the modified Johnson–Cook law (Equation (9)) [29], in which the damage strain ε_f is as follows:

$$\varepsilon_f = \left(D_1 + D_2 e^{D_3 \eta} \right) \left(1 + D_4 \operatorname{Ln} \left(\frac{\dot{\varepsilon}}{\dot{\varepsilon}_0} \right) \right) \tag{9}$$

This description pertains to the fracture strain, accounting for strain rate effects while excluding the thermal term. The different material parameters (D_1 to D_4) are established through experimental characterization tests. The cumulative damage parameter, denoted D , is computed according to the formula presented in Equation (10).

$$D = \sum \left(\frac{\Delta \varepsilon_{pl}}{\varepsilon_f} \right) \tag{10}$$

$\Delta \varepsilon$ is the equivalent plastic strain increment.

When simplifying the damage model to exclude the influences of strain rate and temperature, the fracture strain can be reformulated in terms of stress triaxiality as follows.

$$\varepsilon_f = \left(D_1 + D_2 e^{D_3 \eta} \right) \tag{11}$$

The determination of these constants D_1 , D_2 , and D_3 was established from quasi-static characterization tests on different notched specimens [11]. Subsequently, the strain rate-dependent damage parameter D_4 is determined by considering the dynamic load until strain to fracture occurs. The dataset of strain rate values is examined and their variations in failure strain is interpreted.

4. Friction Models of Blanking Process

In the blanking process, it is essential to account for friction forces, as they significantly affect the prediction of blanking parameters. Friction occurs between the sheet metal and the tool. The contact force F_{fr} (Equation (12)) is divided into two components, which are normal and tangential ones.

$$F_{fr} = F_{fr}^n + F_{fr}^t \tag{12}$$

The external virtual work, which is the sum of the internal virtual work and the inertial work, is expressed by Equation (13). The stress vector is denoted τ .

$$\sum W_{ext} = \int_V f_d \delta U dV + \int_{S_{fr}} \left(F_{fr}^n + F_{fr}^t \right) \delta U dS + \int_{S_\tau} \tau \delta U dS \tag{13}$$

This principle is shown in Equation (14).

$$W_{int} + W_{inert} = \sum W_{ext} \tag{14}$$

The internal virtual work W_{int} and the inertial virtual work W_{inert} are given by relationship (15).

$$\begin{aligned} W_{int} &= \int_V \sigma \delta \dot{U} dV \\ W_{inert} &= \int_V \rho \ddot{U} \delta U dV \end{aligned} \tag{15}$$

Then, the mechanical problem consists in solving the following relationship (16):

$$\int_V \left(\underline{\sigma} : \delta \underline{\varepsilon} + \rho \ddot{U} \delta \dot{U} - f_d \delta \dot{U} \right) dV = \int_{S_{fr}} \left(F_{fr}^n + F_{fr}^t \right) \delta \dot{U} dS + \int_{S_\tau} \tau \delta U dS \tag{16}$$

Once the mathematical equations for a mechanical problem are formulated using external virtual work, it is crucial to select an appropriate friction model. This selection is significant, as different friction models have varying levels of accuracy and applicability in predicting the behavior of mechanical systems. The combined friction model (Equation (17)) is used in blanking process modelling because of its suitability to high stress.

$$\tau_f = \text{Min}(\mu_c \cdot \sigma, \tau_{\max}) \tag{17}$$

We denote τ_f the frictional shear stress, σ the normal contact stress, μ_c the Coulomb coefficient, and τ_{max} the shear flow stress. Figure 3 illustrates the friction models.

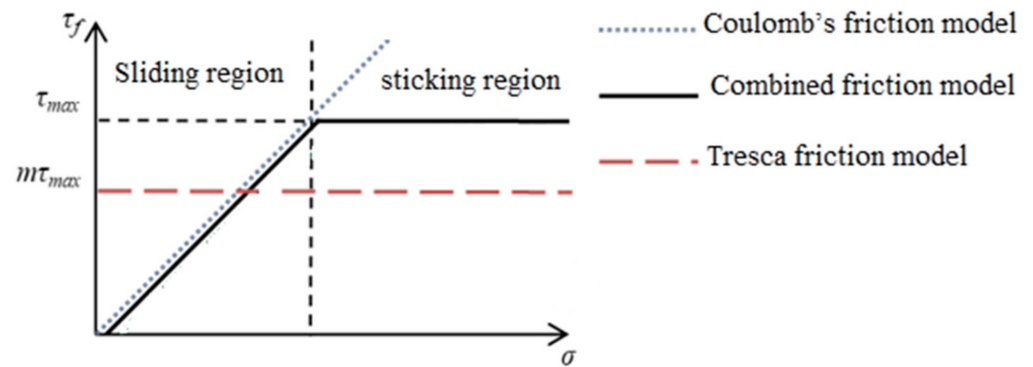


Figure 3. Friction models in blanking process.

For Coulomb’s rule, τ_f increases linearly as a function of σ .

$$\tau_f = \mu_c \cdot \sigma \tag{18}$$

However, for the Tresca friction model, τ_f is proportional to τ_{max} .

$$\tau_f = m \cdot \tau_{max}; 0 \leq m \leq 1 \tag{19}$$

5. Experimental Results of Sheet Blanking Tests

In order to ensure the reproducibility of the blanking test results, these experiments were repeated three times.

Blanking burrs (Figure 4) can be prevented by understanding the influence of the blanking parameters on the design and manufacturing phases during the blanking operation. For that, we study the influence of the sheet thickness, the punch diameter, the blanking speed, and the clearance on the blanking force and the blanked sample profile.

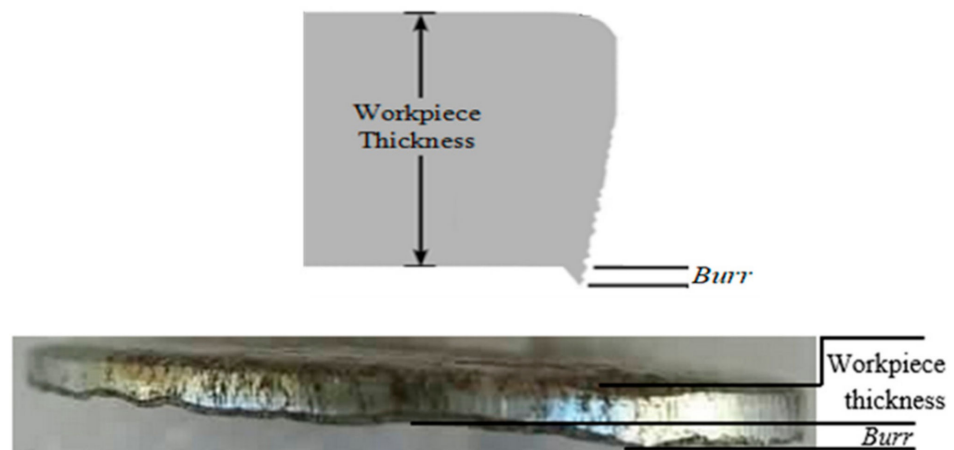


Figure 4. Blanking burr during cutting operation.

Table 3 lists the obtained experimental results.

Table 3. Experimental results of blanking tests.

S_p (mm/min)	J (%)	Th (mm)	D (mm)	Average of Hbv (mm)	Standard Deviation of Hbv (mm)	Average of F_{max} (kN)	Standard Deviation of F_{max} (kN)
20	10	1	14	0.46	0.05	15.33	1.19
40	10	2	14	0.74	0.06	31.87	1.3
40	20	2	14	0.64	0.06	31.61	2.75
20	10	1	18	0.37	0.04	18.55	1.31
40	10	2	18	0.65	0.03	42.16	2.06
40	20	2	18	0.63	0.04	41.91	2.77
40	10	1	18	0.31	0.02	19.25	0.75

In this section, an experimental analysis of burr Hbv and maximum blanking force F_{max} will be presented.

5.1. Experimental Analysis of Hbv

Blanking burr is a phenomenon that allows the control of quality and cost in the blanking process. It is crucial to control aspects of the blanking operation leading to burr appearance. For that, we measure the burr Hbv as a function of the four selected input factors.

From this graph, it can be concluded that the punch speed and the clearance between die and punch affect moderately the average of Hbv . However, an increase in sheet thickness considerably increases Hbv . The punch diameter has a weak influence on Hbv , especially for the case of $Th = 2$ mm, $J = 20\%$, and $S_p = 40$ mm/min. For $Th = 1$ mm, $J = 10\%$, and $S_p = 20$ mm/min, it applies to the data presented in Figures 5 and 6. The effect of punch diameter is clearer, but it remains moderate compared to the effect of sheet thickness on Hbv .

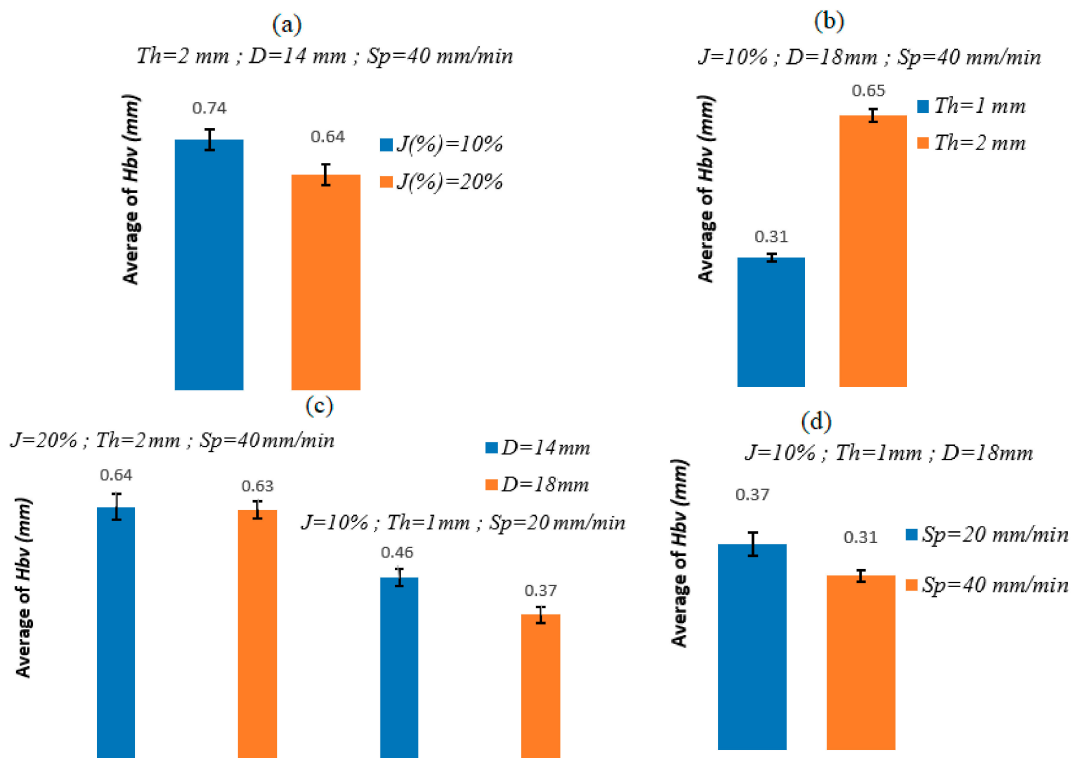


Figure 5. Variation of Hbv as a function of blanking parameters.

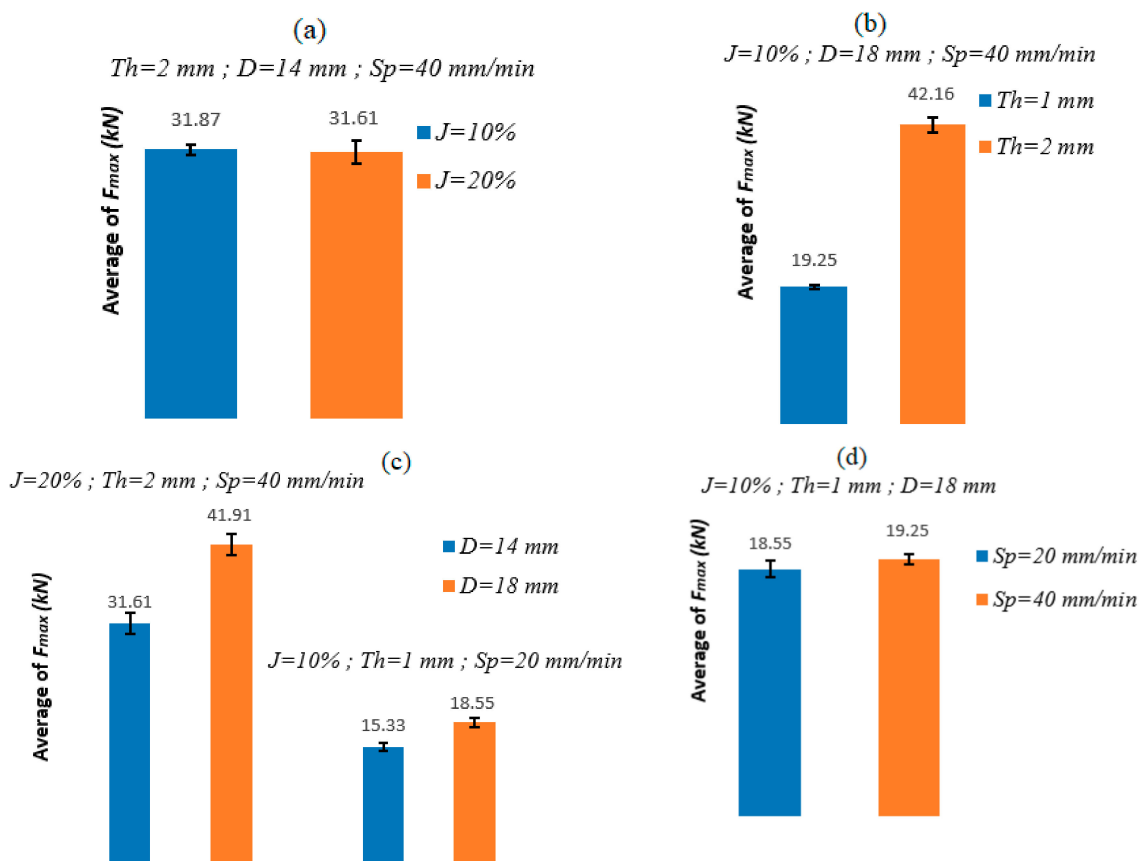


Figure 6. Variation of F_{max} as a function of blanking parameters.

5.2. Experimental Analysis of F_{max}

Knowledge of force evolution in blanking operations is required to predict the fracture mechanisms of sheet metal in a suitable way and to design blanking tools. The maximum blanking force (F_{max}) depends on different blanking parameters such as punch speed, sheet thickness, clearance between punch and die, etc.

From the graph of Figure 6, the increase in thickness and the punch diameter considerably increase F_{max} . The effect of the punch speed and the clearance can be considered negligible.

6. Numerical Study of Sheet Blanking Operation

6.1. Identification of Plasticity and Damage Laws

Tensile tests are experimental procedures utilized to predict mechanical properties and damage parameters. These tests are conducted to ascertain the elastic properties and constants associated with modified Johnson–Cook laws, which elucidate material behavior and damage under high strain rates. In this regard, Figure 7a illustrates the mesh utilized in the numerical simulations of the tensile test. C3D8R elements are employed with a refined meshing zone of $0.5 \times 0.5 \times 0.5\text{ mm}^3$. Figure 7b,c depict the paths along which cracks propagate within the material after experimental and numerical tensile tests conducted at a loading speed of 500 mm/min. Figure 7d illustrates the equivalent plastic strain contour just before failure.

The choice of two different loading speeds is significant because it allows researchers to discern how the material's response varies with different rates of deformation. This is crucial for accurately modeling the material's behavior in the blanking test.

The development of a numerical model for the tensile test simulates the behavior of the material under different conditions, providing a good choice of parameters for the plasticity and damage laws. Figure 8 illustrates the evolution of the true stress curve as a function of true strain. The two loading speeds in the tensile tests are 1 mm/min and 500 mm/min.

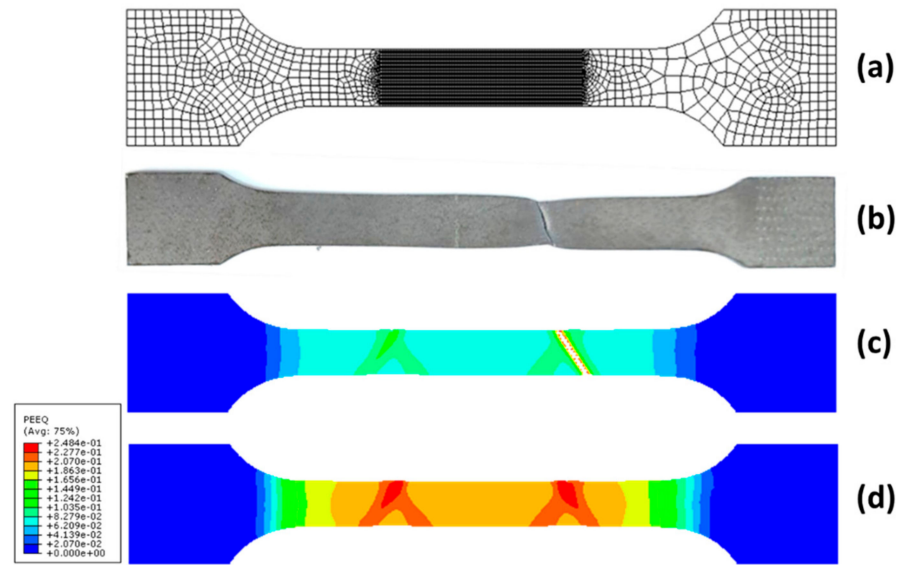


Figure 7. Tensile test specimens: (a) mesh size; (b) experimental test ($V = 500$ mm/min); (c) numerical test ($V = 500$ mm/min); (d) equivalent plastic strain distribution.

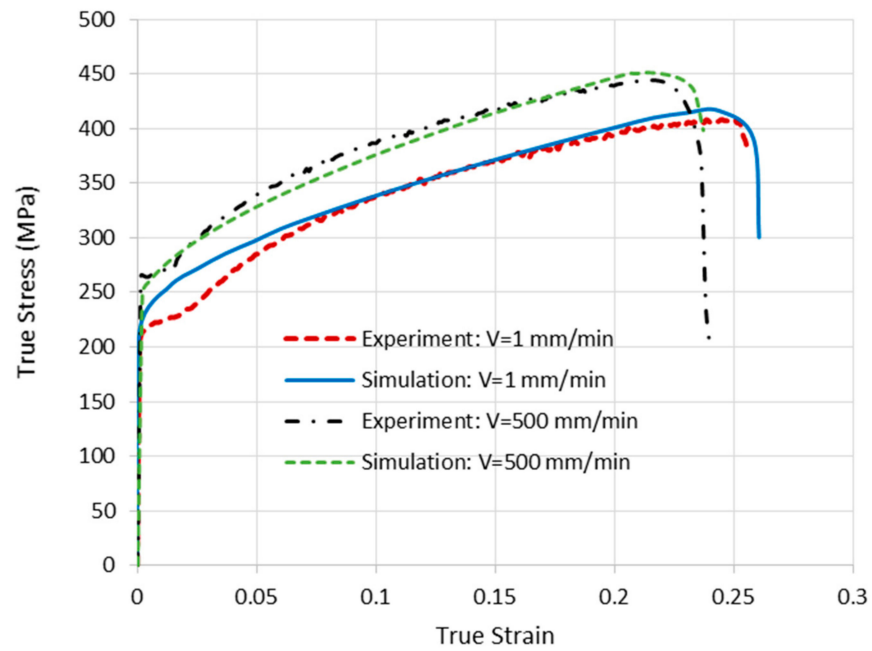


Figure 8. Comparison between predicted and experimental results in tensile test: true stress–strain curve.

A good correspondence between the results indicates that the outcomes obtained from the experimental tests align well with the predictions from the numerical simulations. This suggests that the numerical model accurately predicts the behavior of the sheet metal under different loading conditions. Then the constants of modified the Johnson–Cook model are determined, as shown in Tables 4 and 5.

Table 4. Mechanical properties and plasticity parameters of modified Johnson–Cook model.

E (GPa)	ν	A (MPa)	B (MPa)	n	C	$\dot{\epsilon}_0$
200	0.3	215	510	0.63	0.025	0.00056

Table 5. Damage parameters of modified Johnson–Cook model.

D_1	D_2	D_3	D_4
0.03	0.13	−0.95	0.036

These parameters will be used to simulate the sheet blanking tests.

6.2. Numerical Model of Blanking Operation

A finite element, ABAQUS/Explicit model, is used to compute the blanking process of S235 sheet steel. The meshing utilizes the four-node bilinear axisymmetric quadrilateral element (CAX4R). In our computational model, the die and the punch are assumed to be rigid solids. As shown in Figure 9, a finer mesh is defined in the failure zone.

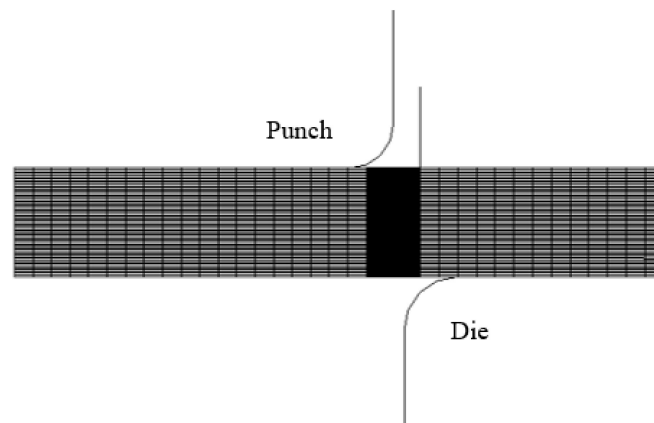


Figure 9. Numerical model sheet blanking operation.

Within this section, the modified Johnson–Cook laws (Equations (3) and (9)) are applied to characterize the yielding behavior and damage of the sheet metal. The combined friction model (Equation (17)) is used in this model. The Coulomb friction coefficient is $\mu_c = 0.3$.

7. Accuracy of the Rate-Dependent Model of Blanking Operations

The numerical model incorporating the rate strain term is utilized to predict the mechanical behavior of S235 sheet steel during blanking operations. Figure 10 presents the computed results.

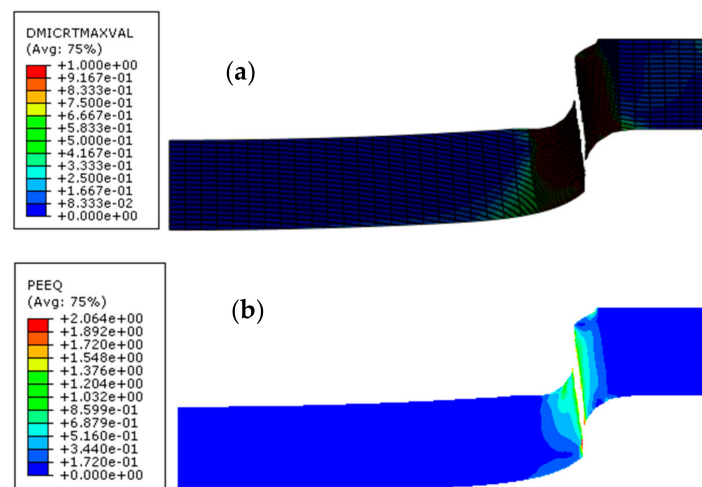


Figure 10. Numerical results: (a) damage fields, (b) strain fields.

In order to analyze the influence of blanking parameters, which are the punch diameter, the clearance, and the sheet thickness, the force–displacement curves are illustrated in the following figures. Specifically, Figure 11 depicts the effect of the sheet thickness, and Figure 12 illustrates the effect of the punch diameter and clearance on the evolution of blanking force and on F_{max} .

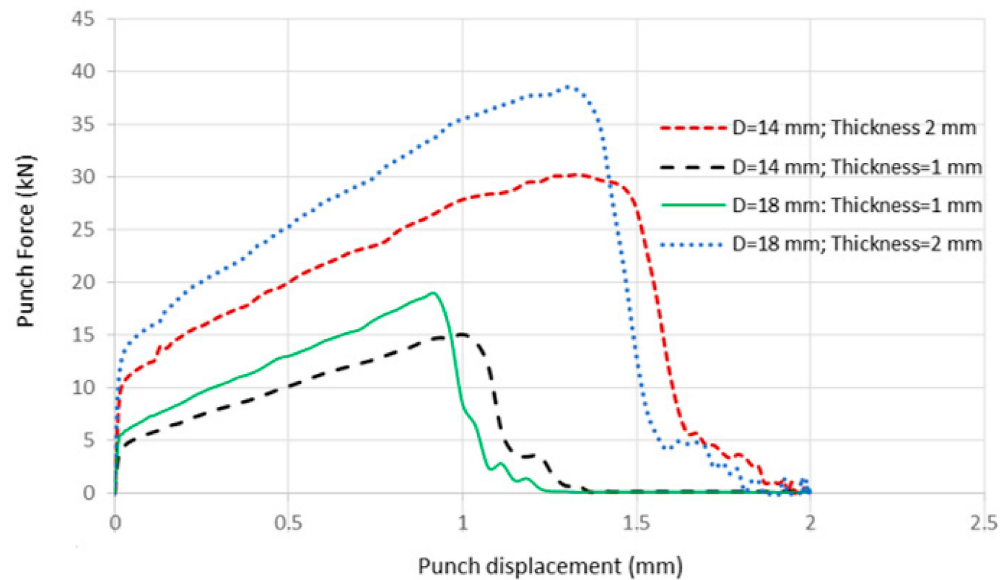


Figure 11. Thickness effect: punch force vs. punch displacement for $j = 10\%$.

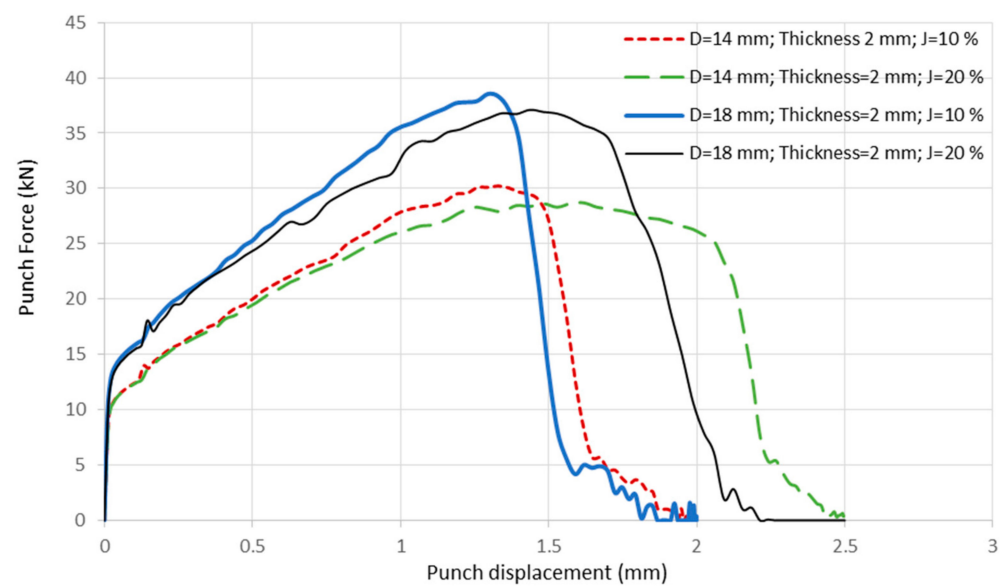


Figure 12. Clearance and punch diameter effects: punch force vs. punch displacement.

The punch force versus punch displacement curves exhibit four distinct phases. Initially, there is the reversible deformation phase, characterized by a linear curve progression. Following this is the irreversible deformation phase with hardening, where the curve continues until reaching the maximum blanking force (F_{max}). Beyond this point, the curve enters the plastic deformation with section reduction phase. Lastly, the curve demonstrates the initiation and propagation of macro cracks in the final zone.

The maximum force, F_{max} , is directly proportional to the sheet thickness. Increasing the sheet thickness leads to a proportional increase in F_{max} and results in increased punch displacement, ultimately causing the part to rupture. However, the effect of punch diameter is less significant compared to sheet thickness. Increasing the punch diameter results in a

slight increase in F_{max} and a slightly quicker rupture. In the same context, the clearance has a negligible effect on F_{max} . This means that variations in clearance do not significantly affect the maximum force required for blanking.

In addition, the second parameter we will analyze is the burr, which is denoted Hbv . This parameter has a notable influence on the exact geometry of the blanked parts. Burr formation can significantly affect the quality and precision of the finished parts, particularly in terms of edge roughness and dimensional accuracy. The computed Hbv (Figure 13) is determined.

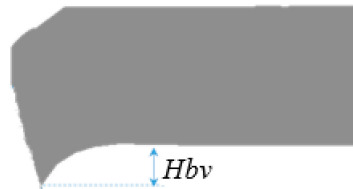


Figure 13. Computed Hbv .

Figure 14 shows the obtained Hbv for different blanking parameters. These results will be compared with experimental results in order to prove the accuracy of numerical model.

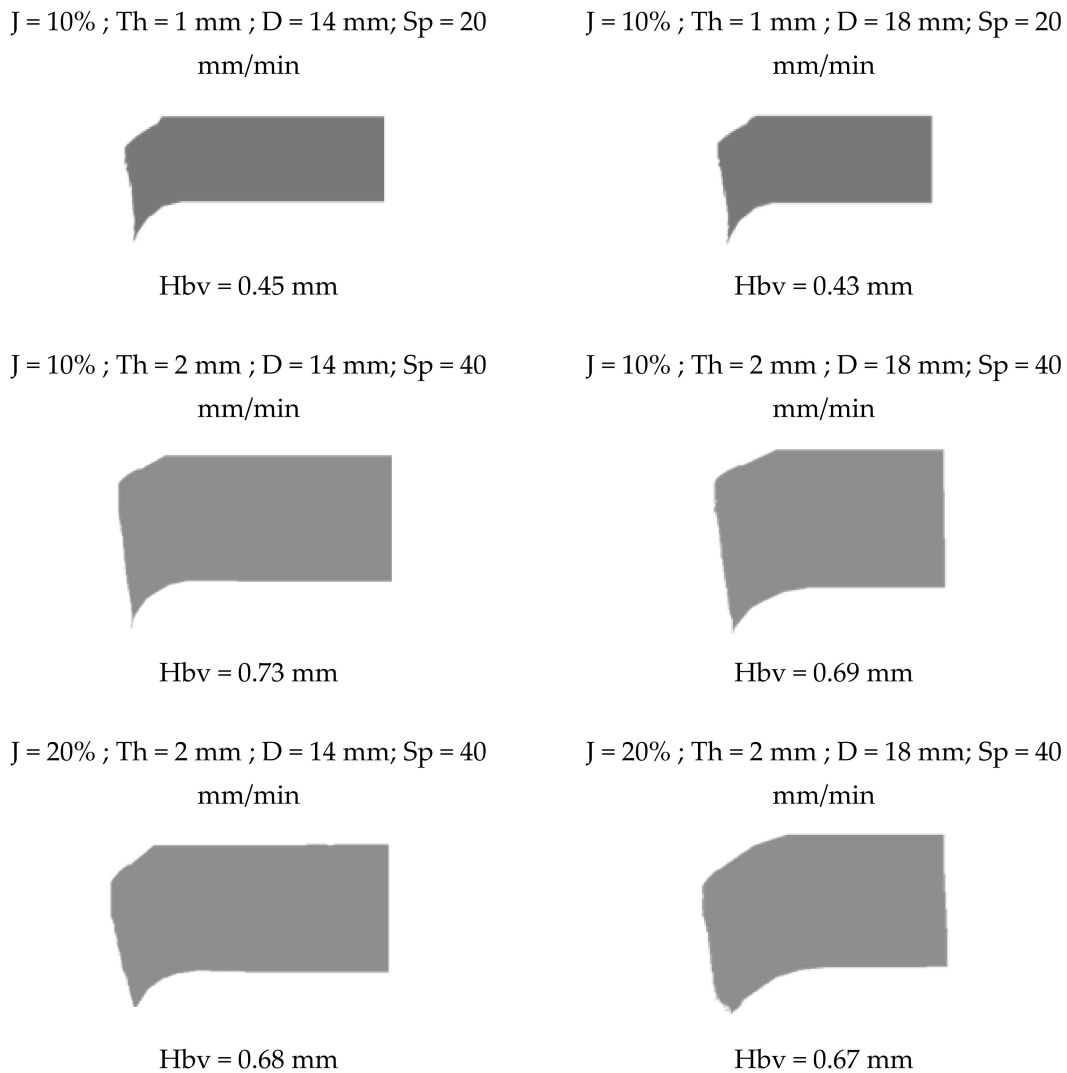


Figure 14. Predicted Hbv with different blanking parameters.

With a high clearance (J) and a high punch diameter (D), the quality of the blanked surface is slightly ameliorated. In addition, the increase in the sheet thickness (Th) gives a worse quality.

Tables 6 and 7 show the comparison between experimental and numerical results in terms of Hbv and F_{max} , respectively.

Table 6. Comparison between Hbv measured and Hbv predicted.

Hbv Measured (mm)	Hbv Predicted (mm)	Error (%)
0.46	0.45	2.17%
0.74	0.73	1.35%
0.64	0.68	6.25%
0.37	0.43	16.21%
0.65	0.69	6.15%
0.63	0.67	6.35%

Table 7. Comparison between F_{max} measured and F_{max} predicted.

F_{max} Measured (kN)	F_{max} Predicted (kN)	Error (%)
15.33	15.10	1.50%
31.87	30.50	4.30%
31.61	28.50	9.84%
18.55	18.65	0.54%
42.16	38.90	7.73%
41.91	37.35	10.88%

A low Error (%) between the Hbv measured and predicted indicates that the numerical model's predictions closely align with the experimental results, signifying high accuracy and reliability in estimating the Hbv values for the blanking test.

A good agreement between the predicted and the experimental results of both blanking parameters proves the accuracy of the developed model in computing the sheet-blanking operation.

8. Conclusions

The main aim of this research is to investigate the effect of the experimental parameters on the workpiece burr (Hbv) and the maximum blanking force (F_{max}). Firstly, a mathematical model for the mechanical aspects of the sheet blanking process was constructed. This model incorporates the modified Johnson–Cook hardening and damage models to characterize the mechanical response of S235 sheet steel. Importantly, it considers the strain rate field generated throughout the blanking process. Secondly, we determined the input factors, which are the punch speed, the punch diameter, the clearance between die and punch, and the sheet thickness that affect the two output measures. Thirdly, the numerical model was developed in order to support numerical and experimental findings. Modified Johnson–Cook models were used in this work. The plasticity law integrates strain hardening and strain rate effects in a multiplicative manner to provide a comprehensive representation of material responses to varying stress conditions. Furthermore, numerical parametric studies were conducted to predict how blanking parameters, in terms of the punch diameter, the clearance, and the sheet thickness, affect the geometrical defects of bar workpieces. These studies examine how the burr evolves and the quality of the sheared surface varies across different blanking parameters values. It was shown that these models exhibited good predictions for the two studied parameters (Hbv and F_{max}).

Author Contributions: L.B.S.: Conceptualization, Methodology, Writing—Original draft preparation. T.K.: Software, visualization, Data curation, investigation. H.H.: Visualization, Writing—Review and Editing, Investigation. M.W.: Supervision, Conceptualization, Methodology, Writing—Review and Editing. All authors have read and agreed to the published version of the manuscript.

Funding: This research received no external funding.

Data Availability Statement: Data are contained within the article.

Conflicts of Interest: The authors declare no conflicts of interest.

References

1. Gohil, A.; Modi, B. Review of the effect of process parameters on performance measures in the incremental sheet forming process. *Proc. Inst. Mech. Eng. Part B J. Eng. Manuf.* **2020**, *235*, 303–332. [[CrossRef](#)]
2. Murugesan, M.; Jung, D.W. Johnson Cook material and failure model parameters estimation of AISI-1045 medium carbon steel for metal forming applications. *Materials* **2019**, *12*, 609. [[CrossRef](#)] [[PubMed](#)]
3. Ben Fraj, B.; Kamoun, T.; Hentati, H.; Trabelsi, M.; Ghazouani, N.; Ahmed, M. Optimization of forming force and Erichsen index using Taguchi design of experiments: Mathematical models and experimental validation. *Proc. Inst. Mech. Eng. Part B J. Eng. Manuf.* **2023**. [[CrossRef](#)]
4. Moakhar, S.; Hentati, H.; Barkallah, M.; Louati, J.; Haddar, M.; Bonk, C.; Behrens, B.A. Modeling of the ductile damage-Application for bar shearing. *Mater. Wiss. Werkstofftech.* **2018**, *50*, 1353–1363. [[CrossRef](#)]
5. Liu, K.; Jin, S.; Rui, Y.; Huang, J.; Zhou, Z. Effect of Lithology on Mechanical and Damage Behaviors of Concrete in Concrete-Rock Combined Specimen. *Mathematics* **2022**, *10*, 727. [[CrossRef](#)]
6. Cazaubon, V.; Abi Akle, A.; Fischer, X. A Parametric Study of Additive Manufacturing Process: TA6V Laser Wire Metal Deposition. In *Advances on Mechanics, Design Engineering and Manufacturing III*; Springer: Cham, Switzerland, 2021; pp. 15–20. [[CrossRef](#)]
7. Hsu, T.J.; Lai, W.H. Manufacturing parts optimization in the three—Dimensional printing process by the Taguchi method. *J. Chin. Inst. Eng.* **2010**, *33*, 121–130. [[CrossRef](#)]
8. Islam, M.N. Effect of additional factors on dimensional accuracy and surface finish of turned parts. *Mach. Sci. Technol.* **2013**, *17*, 145–162. [[CrossRef](#)]
9. Asiltürk, I.; Neşeli, S. Multi response optimisation of CNC turning parameters via Taguchi method-based response surface analysis. *Measurement* **2012**, *45*, 785–794. [[CrossRef](#)]
10. Hambli, R. Design of Experiment Based Analysis for Sheet Metal Blanking Processes Optimisation. *Int. J. Adv. Manuf. Technol.* **2002**, *19*, 403–410. [[CrossRef](#)]
11. Moakhar, S.; Hentati, H.; Barkallah, M.; Louati, J.; Haddar, M. Parametric study of aluminum bar shearing using Johnson-Cook material modeling. *Proc. Inst. Mech. Eng. Part B J. Eng. Manuf.* **2021**, *235*, 1399–1411. [[CrossRef](#)]
12. Meslameni, W.; Ben Salem, C. Modeling of the springback in folding using the experimental design method. *J. Appl. Res. Ind. Eng.* **2021**, *8*, 290–308.
13. Lange, K. *Handbook of Metal Forming*; McGraw-Hill: New York, NY, USA, 1985; ISBN 0-07-036285-8.
14. Zhao, P.J.; Chen, Z.H.; Dong, C.F. Experimental and numerical analysis of micromechanical damage for DP600 steel in fine-blanking process. *J. Mater. Process. Technol.* **2016**, *236*, 16–25. [[CrossRef](#)]
15. Zhou, J.; Gao, X.; Sobotka, J.C.; Webler, B.A.; Cockeram, B.V. On the extension of the Gurson-type porous plasticity models for prediction of ductile fracture under shear-dominated conditions. *Int. J. Solids Struct.* **2014**, *51*, 3273–3291. [[CrossRef](#)]
16. Lemaitre, J. A continuous damage mechanics model for ductile fracture. *J. Eng. Mater. Technol.* **1985**, *107*, 83–89. [[CrossRef](#)]
17. Gurson, A.L. Continuum Theory of Ductile Rupture by Void Nucleation and Growth: Part I—Yield Criteria and Flow Rules for Porous Ductile Media. *ASME J. Eng. Mater. Technol.* **1977**, *99*, 2–15. [[CrossRef](#)]
18. Winter, S.; Nestler, M.; Galiev, E.; Hartmann, F.; Psyk, V.; Kräusel, V.; Dix, M. Adiabatic Blanking: Influence of Clearance, Impact Energy, and Velocity on the Blanked Surface. *J. Manuf. Mater. Process.* **2021**, *5*, 35. [[CrossRef](#)]
19. Moakhar, S.; Hentati, H.; Barkallah, M.; Louati, J.; Bonk, C.; Behrens, B.A.; Haddar, M. Evaluation of AW-6082 Aluminium Bar Shearing Simulation. In *Advances in Materials, Mechanics and Manufacturing*; Springer: Berlin/Heidelberg, Germany, 2020. [[CrossRef](#)]
20. Akyürek, F.; Yaman, K.; Tekiner, Z. An experimental work on tool wear affected by die clearance and punch hardness. *Arab. J. Sci. Eng.* **2017**, *42*, 4683–4692. [[CrossRef](#)]
21. Lawanwong, K.; Pumchan, W. Wear mechanism and ability for recovery of tool steel on blanking die process. *Key Eng. Mater.* **2017**, *725*, 572–577. [[CrossRef](#)]
22. Mucha, J.; Tutak, J. Analysis of the Influence of Blanking Clearance on the Wear of the Punch, the Change of the Burr Size and the Geometry of the Hook Blanket in the Hardened Steel Sheet. *Materials* **2019**, *12*, 1261. [[CrossRef](#)] [[PubMed](#)]
23. Maiti, S.; Ambekar, A.; Singh, U.; Date, P.; Narasimhan, K. Assessment of influence of some process parameters on sheet metal blanking. *J. Mater. Process. Technol.* **2000**, *102*, 249–256. [[CrossRef](#)]
24. Guo, W.; Tam, H.Y. Effects of extended punching on wear of the WC/Co micropunch and the punched microholes. *Int. J. Adv. Manuf. Technol.* **2012**, *9*, 955–960. [[CrossRef](#)]
25. Slavik, J.; Bolka, Š.; Bratuš, V.; Boltežar, M. A novel laboratory blanking apparatus for the experimental identification of blanking parameters. *J. Mater. Process. Technol.* **2014**, *2*, 507–513. [[CrossRef](#)]
26. Hatanaka, N.; Yamaguchi, K.; Takakura, N.; Iizuka, T. Simulation of sheared edge formation process in blanking of sheet metals. *J. Mater. Process. Technol.* **2003**, *140*, 628–634. [[CrossRef](#)]

27. Gréban, F.; Monteil, G.; Roizard, X. Influence of the structure of blanked materials upon the blanking quality of copper alloys. *J. Mater. Process. Technol.* **2007**, *186*, 27–32. [[CrossRef](#)]
28. Johnson, G.R.; Cook, W.H. A constitutive model and data for metals subjected to large strains, high strain rates and high temperatures. In Proceedings of the 7th International Symposium on Ballistics, The Hague, The Netherlands, 19–21 April 1983.
29. Johnson, G.R.; Cook, W.H. Fracture characteristics of three metals subjected to various strains, strain rates, temperatures and pressures. *Eng. Fract. Mech.* **1985**, *21*, 31–48. [[CrossRef](#)]
30. Goijaerts, A.M.; Govaert, L.E.; Baaijens, F.P.T. Experimental and numerical investigation on the influence of process speed on the blanking process. *J. Manuf. Sci. Eng.* **2002**, *124*, 416–419. [[CrossRef](#)]
31. Chan, H.Y.; Abdullah, A.B. Geometrical Defect in Precision Blanking/Punching: A Comprehensive Review on Burr Formation. *RJASET* **2014**, *8*, 1139–1148. [[CrossRef](#)]
32. Fan, W.F.; Feng, L. Study on Blanking Force of Fine-Blanking with Negative Clearance and Common Blanking for AISI-1045 through Simulation and Experiment Methods. *Mater. Sci. Forum* **2011**, *704–705*, 1175–1179. [[CrossRef](#)]

Disclaimer/Publisher’s Note: The statements, opinions and data contained in all publications are solely those of the individual author(s) and contributor(s) and not of MDPI and/or the editor(s). MDPI and/or the editor(s) disclaim responsibility for any injury to people or property resulting from any ideas, methods, instructions or products referred to in the content.